BIOSILICA-DRIVEN INNOVATION: A VALORIZATION APPROACH TO CIRCULAR BIO-BASED MATERIALS

Filipa Gomes[1], Sara Gomes[1], Juliana Oliveira[1], Mariana Ornelas[1], José Gonçalves[2], Pedro Costa[2]
[1]CeNTI - Centre for Nanotechnology and Advanced Materials, Rua Fernando Mesquita 2785, 4760-034 Vila Nova de Famalicão, Portugal; fgomes@centi.pt; mornelas@centi.pt
[2] Biofabics Lda – Rua Alfredo Allen 455, 4200-135 Porto, Portugal; pedro.costa@biofabics.com; jose.goncalves@biofabics.com

ABSTRACT: Agroindustrial residues are abundant, low-cost sources for high-value bio-based products. This work was developed within the PRIMED project (GA N°101135353, HORIZON-CL6-2023-CIRCBIO-01), which co-creates circular business models to integrate primary producers into bioeconomy value chains by enabling the valorization of waste and by-products. CeNTI's Bio-silica Lab (Portugal) focuses on extracting and surface-tailoring silica from rice husk to produce value-added multifunctional particles. A circular valorization pathway that integrates these particles into electrospun polymer nanofibers is presented as a case study, validating their use in real scenarios. The silica recovered from rice husk was modified to confer antimicrobial activity, hydrophobicity and flame resistance, and the particles were incorporated into polymer solutions and processed into nanofibrous meshes by electrospinning after optimizing solution properties and processing parameters. By converting a passive filler into a tunable, multifunctional additive derived from a widely available residue, this study links circular-economy materials to high-value applications and reduces dependence on non-renewable additives.
Keywords: agroindustrial residues, biomaterial, green chemistry, industry, recycling, rice husks, sustainability, waste

1 INTRODUCTION

Agroindustrial residues are an abundant, low-cost feedstock for producing high-value bio-based materials. Nowadays, waste management comes as a global challenge, with resource efficiency and decarbonization being the most assertive solutions to help create a greener and more sustainable world [1–3]. Specifically, rice husk (RH) is an abundantly available waste material in all rice producing countries, with China and India being the countries with the highest production in the last 10 years, of around 42.54 and 33.70 million tons, respectively, in a total of 153.95 million tons [4]. Consequently, RH is one of the most abundant residues of the agro-industry and produces, when incinerated, the highest percentage of ash (23 %), compared to other waste from cereals, such as sugarcane bagasse (15 %), corn leaves, and wheat (12 % and 10 %, respectively) [5]. Due to its high availability and the high percentage of silica [6] (typically around 90 %), the RH ash has latent potential for being reused as a secondary raw material to produce silica-based materials for different applications, such as drug delivery [7], biomedical [8], optical devices [9], catalysis [10], agriculture [11] or in the production of value-added ceramics [12].

The precipitation method has been widely described to produce highly pure nanosilica, a method that typically uses the alkali extraction of RH ash to obtain silicate, followed by its precipitation using an acidic solution, such as hydrochloric, nitric or sulphuric acid [13, 14].

Also, through simple chemical treatments, different functional groups can be easily incorporated on the silica surface, enhancing its properties. Environmentally friendly pathways for the functionalization of biosilica can be accomplished with the use of bio-based compounds such as phosphorous-based groups or quaternary ammonium salts with silane groups, to impart multifunctional properties such as flame retardancy, antifungal, and hydrophobicity. Silanes groups introduced in quaternary ammonium compounds are interesting compounds for the functionalization of silica particles, through sol-gel technology. Song *et al.* (2011), for example, functionalized silica particles with an ammonium chloride silane called 3-(trimethoxysilyl)-propyldimethyloctadecyl ammonium chloride (QAS) [15]. The authors compared QAS-silica nanoparticles with silica nanoparticles functionalized with octadecyltrimethoxy silane (OdS). Both modifications exhibited similar hydrophobicity, but QAS-modified silica showed better results when compared to OdS-modified silica in reducing the growth of bacteria [15]. Gong *et al.* (2014) have also reported one-pot modification of silica particles with QAS and 3-methacryloxypropyltrimethoxysilane; these particles, when incorporated into bis-GMA/TEGDMA resin, exhibited antimicrobial activities against *Streptococcus mutans*, *Actinomyces naeslundii*, and *Candida albicans* [16]. Wang and co-workers (2017) also prepared a layer-structured montmorillonite nanocomposite containing QAS-grafted silica nanoparticles that exhibited an excellent antibacterial capability against Gram-negative and Gram-positive bacteria [17]. Many of the works reported for the use of QAS for antimicrobial features are related to the preparation of coatings in textile substrates. Tomšič *et al.* (2014), for example, developed antifungal and antibacterial textiles promoted by the application of QAS. The results suggested that the increase in the concentration of QAS enhanced the antimicrobial protection of fibres. Additionally, the authors observed that the antimicrobial activity of QAS is affected by the type of fibre, exhibiting better results for cotton than those obtained for wool and silk fibres [18]. Works from Vasiljevic *et al.* (2017) have also described the use of QAS to develop one- [19] and multi-component coatings [20] for cellulose fibers that were able to reduce the growth of the bacteria *Escherichia coli* and *Staphylococcus aureus* [20]. Riaz and co-workers prepared a cotton textile (by dry-padding) loaded with (3-Glycidoxypropyl)trimethoxysilane and QAS-modified silica nanoparticles, enhancing cotton's hydrophobicity and antibacterial activity, which are durable up to 20 industrial washing cycles [21].

Additionally, several studies reported developments of organic-inorganic compounds by using silane agents, such as tetraethoxysilane (TEOS, precursor of silica) and phytic acid (PA), envisioning flame-retardant properties.

Cheng *et al.* (2020) developed a PA/silica organic-inorganic hybrid sol by using TEOS as a silica precursor. PA was used to enhance the flame retardancy properties of cotton fabrics, where sodium alginate was applied as an anti-agglomeration agent and stabilizer for the hybrid silica sol-gel and citric acid as a cross-linking agent that promoted the interaction between alginate and cotton fiber [22]. Also, Barbalini *et al.* (2019) developed a sol-gel hybrid organic-inorganic coating based on PA and TEOS with different ratios to enhance the flame-retardant properties in cotton fabrics [23]. Sui *et al.* (2020) developed a flame-retardant system for epoxy resin composed of 3D organic-inorganic core-shell nanoparticles, with aminated silica nanoparticles post functionalized with PA and nickel (nickel phytate complex) [24]. The incorporation of the modified particles has improved the thermal stability of the resin. Fu *et al.* (2019) also reported a coating with hydrophobic and flame-retardant properties for cotton fabric composed by bilayer of chitosan/PA and subsequently a layer of hydrophobic silica nanoparticles [25].

One of the examples of this valorization was the development of electrospun polymer nanofibers, incorporating multifunctional biosilica reported herein. Electrospinning has emerged as one of the most versatile and scalable techniques to produce micro- and nanofibrous materials with high specific surface area, interconnected porosity and tunable surface properties. These features make electrospun materials particularly attractive for biomedical, filtration, healthcare, and advanced textile applications, where control over wettability, bioactivity, mechanical performance and mass transport is required [26, 27]. In particular, electrospun structures can closely mimic the architecture of the extracellular matrix (ECM), promoting cell adhesion, proliferation, and nutrient diffusion, which explains their increasing use in tissue engineering and wound-healing systems [28, 29].

The incorporation of inorganic nanoparticles into electrospun polymeric matrices has also gained significant attention as a strategy to impart multifunctionality to nanofibrous systems. Silica nanoparticles are especially relevant due to their high surface area, chemical stability, biocompatibility, and ease of surface functionalization [30, 31]. Several studies have demonstrated that silica-containing electrospun fibers may improve mechanical reinforcement, thermal stability, antimicrobial performance and surface wettability, depending on the particle chemistry and polymeric matrix employed [32–34].

More recently, the use of bio-derived silica obtained from agro-industrial residues has attracted interest as a sustainable alternative to conventional synthetic silica, contributing simultaneously to waste valorization and the development of circular material platforms [35]. However, despite the growing interest in biosilica production and functionalization, the integration of multifunctional rice-husk-derived biosilica into electrospun nanofibers remains scarcely explored, particularly regarding the combination of antimicrobial, hydrophobic, and flame-retardant functionalities within the same fibrous structure.

This work was carried out within the PRIMED project (GA N°101135353, HORIZON-CL6-2023-CIRCBIO-01), which seeks to co-create innovative forms of cooperation to integrate primary producers into bioeconomy value chains. By doing this, PRIMED will enable primary producers to valorize waste and by-products, creating alternative revenue streams. The project aims to develop circular business models in bioeconomy to produce, in biorefineries, bio-based high-value products.

Briefly, the aim of this work was to develop and validate a scalable process that incorporates rice-husk-derived silica into electrospun nanofibers while preserving and enhancing particle functionality. The approach comprised three sequential steps:

(1) Controlled extraction of silica from rice-husk ash using alkaline digestion.

(2) Chemical surface modification of the bio-silica with a quaternary ammonium silane and a phosphorus-containing flame-retardant agent to confer antimicrobial, hydrophobic and flame-retardant properties, followed by physicochemical and functional characterization.

(3) Incorporation of the modified particles into value-added products, such as polymer solutions to produce nanofibers performance by electrospinning.

2 MATERIALS AND METHODS

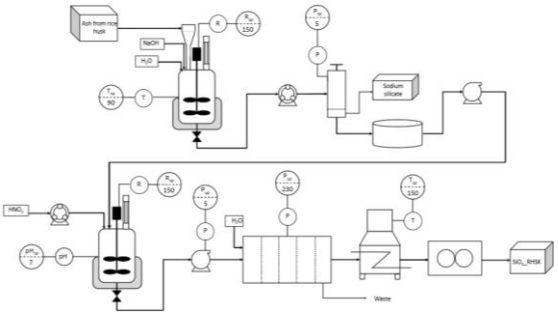
2.1 Materials

Rice husk (RH) was obtained from Arrozeiras Mundiarroz, S.A. (Coruche, Portugal). Nitric acid (65%, PA) and sodium hydroxide were purchased from ChemLab and Fisher Chemical, respectively.

Dimethyl-octadecyl [3-(trimethylsilyl)propyl] ammonium chloride solution (QAS) 42 wt.% in methanol was purchased from Sigma-Aldrich (Schnelldorf, Germany). Inositol hexa-phosphoric acid (phytic acid, PA; 50 wt.% aqueous solution) was obtained from Acros Organics (Geel, Belgium). Absolute ethanol (EtOH) was purchased from Aga (Prior Velho, Portugal). Ultra-pure water of Milli-Q quality (Millipore, Italy) was used. All other re-agents used were of analytical grade.

2.2 Biosilica extraction

Non-modified silica particles (SiO_2_RHSK) were recovered from rice husk.



Scheme 1: Alkaline digestion of rice husk followed by a neutralization step with nitric acid – pilot scale reactor with a filter press.

Briefly, the husk was digested in an alkaline medium, followed by precipitation of the dissolved silicates with nitric acid. Scheme 1 illustrates the procedure that was adapted from the work described by Aguilar *et al.* (2019) [36]. A continuous system was used with a 100 L reactor connected to a filter press. A pilot muffle furnace was

used both for RH ash production and the drying step of SiO_2_RHSK.

The inputs and outputs of this extraction are summarized in Table I.

Table I: Inputs and Outputs for **SiO_2_RHSK.**

Input/Output	Amount
RH Ash	2.4 kg
NaOH	40 L
Solid waste (wet)	1295 g
HNO_3	Around 20 L
SiO_2_RHSK (wet)	8.7 kg
SiO_2_RHSK (dry)	2.1 kg

2.3 Hydrophobic and Multifunctional Biosilica – functionalization steps

A specific amount of the SiO2_RHSK produced was, as previously mentioned, further modified targeting different functional properties.

2.3.1 Hydrophobic silica particles (SiO_2_RHSK_HP)

To achieve hydrophobic properties (SiO_2_RHSK_HP), octadecyltrimethoxysilane (C18) was used for the modification of the particles' surface. It is possible to see the inputs and outputs of this process in Table II.

Table II: Inputs and Outputs for SiO_2_RHSK_HP.

Input/Output	Amount
SiO_2_RHSK	30 g
EtOH	4.8 L
HCl	750 mL
EtOH:C18	1200 mL
SiO_2_RHSK_HP (wet)	900 g
SiO_2_RHSK_HP (Dry)	360 g
SiO_2_RHSK_HP (Grinding)	350 g

Table III: Inputs and outputs **for SiO_2_RHSK_MF.**

Input/Output	Amount
SiO_2_RHSK	70 g
EtOH	2.1 L
H_2O	2.1 L
PA	2.8 L
QAS	875 mL
SiO_2_RHSK_MF (Wet)	2752 g
SiO_2_RHSK_MF (Dry)	514 g
SiO_2_RHSK_MF (Grinding)	497 g

Regarding the multifunctional particles (SiO_2_RHSK_MF – hydrophobicity, flame retardancy and antimicrobial activity), the functionalization of the particles was achieved with Inositol hexaphosphoric acid (PA) and Dimethyl-octadecyl [3-(trimethoxysilyl)propyl] ammonium chloride solution (QAS). It is possible to see the inputs and outputs of this process in the Table III.

2.4 Electrospinning of Biosilica-loaded nanofibers

Electrospun nanofibrous meshes incorporating biosilica particles were produced using a needleless electrospinning system (NEUNEX RespinBot MINI). The equipment was operated with positive and negative high-voltage power supplies to generate a stable electric field and promote the formation of polymeric jets.

Different polymeric systems were evaluated according to the intended final application, including polyvinyl alcohol (PVA), polycaprolactone (PCL), polyamide 6 (PA6), polyurethane (PU), polyvinyl butyral (PVB), and collagen/pullulan blends. Biosilica particles (SiO_2_RHSK, SiO_2_RHSK_HP and SiO_2_RHSK_MF) were dispersed in compatible solvent systems using ultrasonic homogenization before incorporation into the polymer solutions. The final biosilica content in the electrospinning formulations was adjusted according to polymer processability and fiber stability. Depending on the polymer-solvent system, electrospinning was performed using either a top-filled linear blade electrode or a bottom-filled linear cleft electrode. Processing parameters, including voltage, spinning distance, solution feed rate and collector configuration, were optimized for each formulation to obtain stable jet formation and homogeneous nanofibrous structures. For aqueous systems, electrospinning was typically performed using voltages up to +70 kV/-30 kV and a working distance of approximately 370 mm. Organic solvent-based systems were processed using top-filled blade electrodes with working distances between 250 mm and 270 mm. Nanofibers were collected on polypropylene spunbond substrates (40 g/m^2) or metallic collectors. Attention was given to fiber uniformity, particle dispersion, formation of aggregates and preservation of nanofibrous architecture after biosilica incorporation.

2.5 Physical and Chemical Characterization

The physical and chemical characteristics of the produced biosilica particles and electrospun fibers were assessed by using various relevant techniques, as well as the functional properties, as detailed in the following subsections:

a) Attenuated total reflectance (ATR) Fourier transform infrared (FTIR) spectroscopy (FTIR-ATR)

FTIR-ATR was used to evaluate the functional groups of the synthetized particles using a Perkin Elmer Spectrum 100 Series spectrophotometer with a spectral range and resolution factor of 4000 to 650 cm^{-1} and 8 cm^{-1}, respectively.

b) Dynamic light scattering (DLS)

Zeta potential measurements in DLS analysis were performed with a Zetasizer Nano ZS90 (Malvern) and a disposable capillary cell (DTS1070) at 25 °C. For measurements, SiO_2_RHSK, SiO_2_RHSK_HP and SiO_2_RHSK_MF were dispersed in ethanol at a concentration of 1 g/L and subjected to ultrasonic stirring (30 minutes) before the analysis.

c) Thermogravimetric analysis (TGA)

TGA was performed on a TG 209 F1 Libra apparatus (Netzsch) with a Top-loading type of thermobalance. The analysis was carried out by an internal method "Evaluation of the thermal stability of materials by thermogravimetry" based on the standard ISO 11358:1997(E). The samples were pre-conditioned at laboratory's ambient conditions: room registered temperature (≈ 23 °C) and relative humidity (≈ 51 %). For the sample pre-treatment, each one was properly separated, to fit inside the crucible (volume of 85 µL) and to ensure maximum contact with its bottom. The tests were accomplished in a synthetic air atmosphere, following a temperature program from 30 to 700 °C, with a heating rate of 20 ºC/min.

d) XRF analysis

Elemental analyses were performed using an X–550 portable energy dispersive X-ray fluorescence spectrometer (EDXRF) (SciAps Inc., USA). This equipment features an X-ray tube with a gold (Au) anode that operates at a maximum voltage of 55 kV and a maximum current of 200 µA, as well as a high-resolution silicon drift detector (SDD). Measurement acquisition time was approximately 30 seconds per point in an ambient atmosphere. Elemental identification and quantification were obtained using the instrument's internal calibration algorithms, which were implemented in the software.

e) Morphological analysis

The morphology and elementary analysis of the reclaimed material were conducted with the use of Scanning Electron Microscope (SEM) (Phenom Pharos G2, Thermo Scientific) – Schottky Field Emission Source (maximum resolution < 2 nm) with a software Phenom User Interface and equipped with three detectors: Backscattered (BSD), Secondary electrons (SED) and Energy-Dispersive X-ray Spectroscopy (EDS) for semi-quantitative analysis. Previously, the sample was prepared with carbon tape followed by a sputtering treatment for each sample, using a platinum target with a thickness of 5 nm. The EDS analysis was conducted at a magnification of 650 x, using a BSD Full detector and low vaccum (60 Pa) under the acceleration voltage of 15 kV in a mapping mode, or local mode.

f) Tensiometry (contact angle analysis) – hydrophobic properties

The water contact angle measurements of the particles were determined with a tensiometer (Attension Theta, Biolin Scientific) through the sessile drop method, with a water droplet volume of 3 µL, using the OneAttension software. The contact angle measurements were performed on circular pellets (3.5 cm in diameter), prepared with 4/5 g of particles and using a PELA-9040 Powdered Sample Press.

g) Flammability tests – flame retardant properties

The flammability behavior of the functionalized CO textile fabrics samples (SiO_2_RHSK and SiO_2_RHSK_MF) was determined by measuring the flame spread properties of a vertically oriented cotton fabric (560 x 170 mm) according to ISO 6941:2013. Textile substrates were used to facilitate the evaluation of particle behavior. The source ignition was applied on the surface of the cotton fabric (at 90°) and exposed to the flame for 10 s. After the flame source was removed, the propagation times of the flame in the cotton textile were recorded.

h) Antimicrobial tests

To evaluate the minimum concentration of SiO_2_RHSK_MF that has an inhibitory effect on the growth of microorganisms, LBA growth media were prepared with SiO_2_RHSK_MF at concentrations of 20 and 30 mg/mL. The media, already prepared with functionalized silica, were autoclaved to reduce contamination caused by the silica. Once the plates were ready, 10 µL drops of *E. coli* and *S. aureus* inoculum were placed on the respective plates, and these were placed in an incubator at 37 °C for 24 h.

i) Characterization of polymer solutions for electrospinning

Polymer solutions containing silica particles were characterized regarding viscosity (ViscoStar-II differential viscometer), conductivity and pH to assess their suitability for electrospinning processing and to optimize stable jet formation.

j) Electrospun fibers morphological analysis

The morphology of electrospun nanofibrous meshes was evaluated by scanning electron microscopy (SEM) using a desktop SEM (Phenom-World). Before imaging, samples were sputter-coated using an SC7620 Mini Sputter Coater/Glow Discharge System (Quorum Technologies) to improve surface conductivity and image quality. The analyses were performed to evaluate fiber morphology, fiber diameter distribution, structural homogeneity, particle dispersion within the polymeric matrix, and the presence of structural defects such as bead formation or particle agglomeration.

k) Wettability, Stability and Degradation analysis

The wettability meshes was assessed through water contact angle measurements using an Attension Theta tensiometer (Biolin Scientific). Water droplets with a volume of 3 µL were deposited onto the sample surface and analyzed using OneAttension software. The structural stability was evaluated by degradation studies under aqueous conditions (≈22 °C). Structural integrity and dissolution behaviour were monitored over a period of up to 7 days. For water-soluble polymer systems, namely polyvinyl alcohol (PVA)-based formulations, a crosslinking treatment was performed at 60 °C for 48 h using glyoxal and phosphoric acid as crosslinking agents to improve structural stability and reduce dissolution.

3 RESULTS AND DISCUSSION

Figure 1 shows the FTIR spectra of SiO_2_RHSK, SiO_2_RHSK_HP and SiO_2_RHSK_MF.

Concerning SiO_2_RHSK_MF, the presence of characteristic peaks of C-H stretching and deformation vibration bands at 2917 cm^{-1}, 2852 cm^{-1}, and 1467 cm^{-1} are related to QAS [37] and the broad band at 2114 – 2480 cm^{-1} corresponds to the OH—P=O groups from PA [38]. Similar peaks near to 2000 cm^{-1} in SiO_2_RHSK_HP are also related to C-H stretching. As expected, the spectra for all SiO_2_RHSK (with and without functionalization) exhibited bands at 802 cm^{-1} and 1059 cm^{-1}, which could be assigned to the symmetric and asymmetric stretching vibration of Si-O-Si bonds, respectively [39]. Additionally, a band at 1647 cm^{-1} can be observed, which appears in all spectra except for SiO_2_RHSK, and that is being attributed to absorbed H_2O [40].

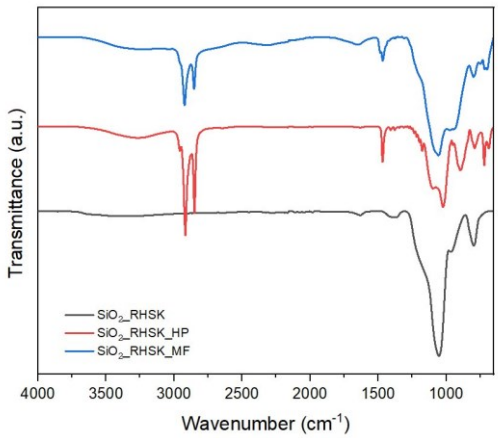


Figure 1: FTIR spectra for the samples: SiO_2_RHSK, SiO_2_RHSK_HP and SiO_2_RHSK_MF.

The thermogravimetric analysis (TGA) of SiO_2_RHSK, SiO_2_RHSK_HP and SiO_2_RHSK_MF is shown in Figure 2. In SiO_2_RHSK no degradation of material is observed in the range of 200 – 500 ºC. In this case, the particles only have inorganic composition (a residual mass higher than 95 %). On the other hand, for HP and MF modifications, there are different weight losses corresponding to C18, PA and QAS. At the end, in both particles, a residual mass of 25 – 40% was obtained.

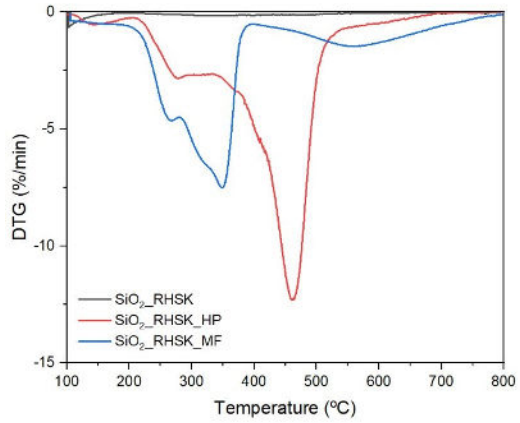


Figure 2: DTG curves obtained at 20°C/min under a dynamic synthetic air atmosphere for the samples: SiO_2_RHSK, SiO_2_RHSK_HP and SiO_2_RHSK_MF.

These results are in accordance with the ones obtained using other techniques, namely XRF and EDS analysis, with a higher relative standard deviation for EDS analysis, a semi-quantitative approach (Table IV).

Table IV. Weight concentration (%) obtained by XRF and EDS analysis

Sample	XRF	EDS
SiO_2_RHSK	Si = 35 ± 6	Si = 40 ± 4
SiO_2_RHSK_HP	Si = 22 ± 2	Si = 21 ± 10
SiO_2_RHSK_MF	Si = 15 ± 1 P = 11 ± 1	Si = 8 ± 5 P = 8 ± 3 N = 4 ± 1 Cl = 2 ± 1

Finally, the morphology of the particles was evaluated. The SiO_2_RHSK particles exhibited a spherical morphology in the range of 50-80 nm but with agglomerated structure (clusters of nanoparticles). However, in HP and MF particles, the morphology changed to a more laminated status, as also demonstrated by Gong *et al.* (2014) [41].

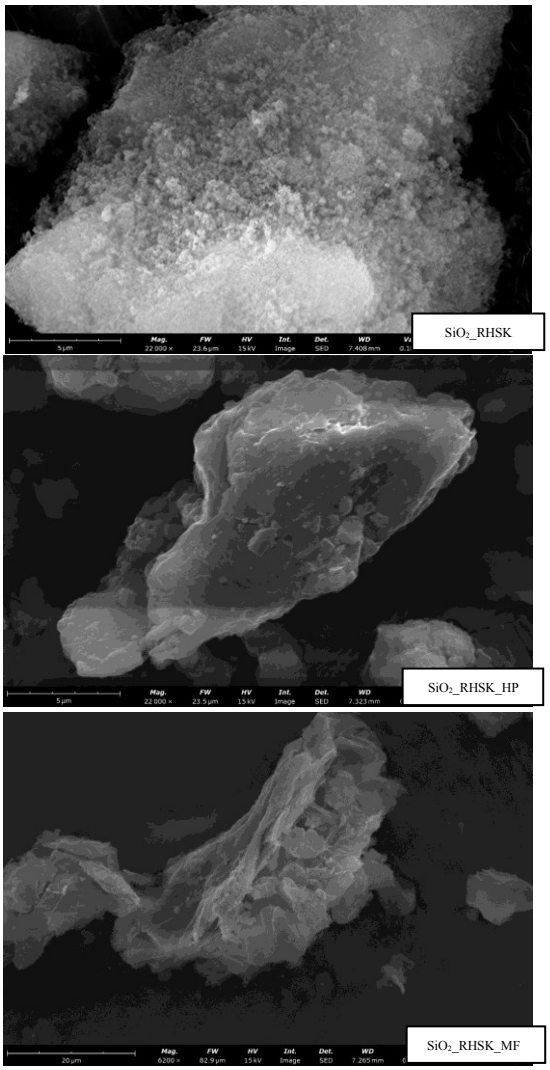


Figure 3: SEM images for the samples: SiO_2_RHSK, SiO_2_RHSK_HP and SiO_2_RHSK_MF.

Zeta potential through DLS analysis was studied, and SiO_2_RHSK and SiO_2_RHSK_HP showed a negative charge of -27.6 ± 0.8 mV and -13.3 ± 0.9 mV, respectively. As expected, SiO_2_RHSK_MF increased the zeta potential to a more positive value of 40 ± 1 mV, in line with what was previously reported by Wang *et al.* (2017) [42].

Due to the well-known water repellent properties of the long-chain alkyl silanes and QAS (with an 18 C chain), the hydrophobic behavior of the modified particles was also assessed by water contact angle (WCA) measurements. The WCA of SiO_2_RHSK_HP (119 ± 8 º) and SiO_2_RHSK_MF (100 ± 7 º) increased when compared to SiO_2_RHSK (49 ± 9 º). The functionalized particles exhibited hydrophobic properties (θ>90°) and are in line with those reported in the literature for similarly functionalized particles [43, 44].

Figure 4 shows the scheme used in the flame retardancy behavior according to the ISO 6941:2003 (vertical burning – A), as well as the photographs of the test performed for the SiO_2_RHSK (B) and SiO_2_RHSK_MF (C) particles. Due to the existence of an "external" element that was used to facilitate the impregnation of particles such as the textile, two different assays were also accomplished: cotton with (D) and without chitosan (E). Almost the whole samples, except (C), were completely burned (10 s. of ignition time pre-established in ISO 6941:2003), which results in a total char length of about 51.0 cm. SiO_2_RHSK_MF particles exhibited a good char formation, and the flame self-extinguished after the ignition time (with a char length <11 cm) – Figure 4 (F).

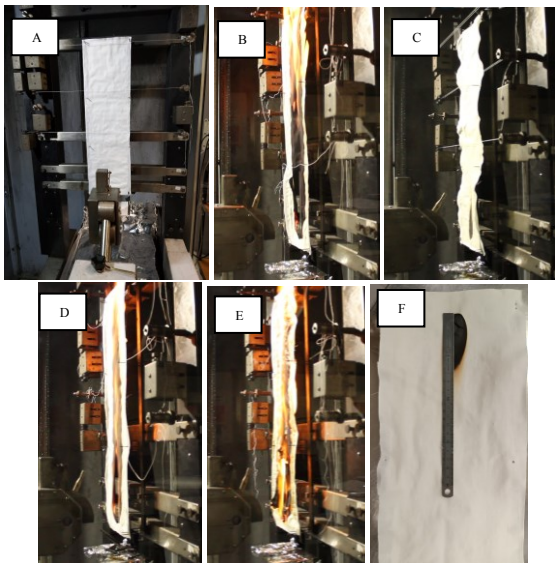


Figure 4: ISO 6941:2003 vertical burning tests for cotton with (B) SiO_2_RHSK and (C) SiO_2_RHSK_MF and cotton with (D) 3% chitosan (in acetic acid w/v) and (E) without.

Furthermore, as it is possible to observe in Figure 5, SiO_2_RHSK_MF particles were able to reduce the growth of *E. coli* and *S. aureus* with a MIC > 30 mg/mL, while SiO_2_RHSK particles continued to promote the bacteria's growth.

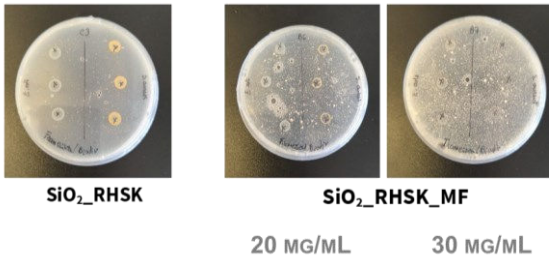


Figure 5: The concentration of *E. coli* and *S. aureus* after 24 h of incubation with SiO_2_RHSK_MF particles (5 replicates per sample). SiO_2_RHSK was used as a control.

The incorporation of SiO_2_RHSK_MF into electrospun polymeric matrices enabled the development of application-oriented nanofibrous systems with distinct functional profiles.

Hydrophilic silica incorporated into nanofibrous meshes promoted increased wettability. It may contribute to improved cell-material interactions, which is particularly relevant for tissue engineering and *in vitro* cell culture applications. In contrast, hydrophobic and antimicrobial SiO_2_RHSK variants enabled the development of protective fibrous barriers with potential use in wound dressings, filtration systems and technical textiles.

PVA- and PU-based nanofibrous meshes containing SiO_2_RHSK demonstrated promising characteristics for healthcare-related applications, particularly due to the combination of high porosity, flexibility and antimicrobial activity.

Collagen/pullulan nanofibrous meshes incorporating SiO_2_RHSK particles showed modifications in fiber architecture after particle incorporation. SEM analysis demonstrated the formation of more open and fluffy structures, while some formulations exhibited increased fiber fragmentation and particle aggregation. Among the evaluated systems, SiO_2_RHSK_MF showed the lowest impact on fiber morphology, suggesting improved compatibility and dispersion within the polymeric matrix. The rapid dissolution characteristics of collagen/pullulan systems support their potential application in dissolvable cosmetic patches and topical delivery systems. PVA-based nanofibrous meshes incorporating silica particles were successfully produced under stable electrospinning conditions. SEM analysis indicated the presence of bulged structures suggesting encapsulation of silica particles within the polymeric fibers. Furthermore, crosslinked formulations maintained structural integrity during aqueous degradation studies for up to 7 days, demonstrating improved stability compared to non-crosslinked systems. These characteristics support the potential use of PVA-based systems in healthcare-related applications, particularly where controlled stability and high porosity are required. Hydrophilic silica particles incorporated into PCL nanofibers resulted in a reduction of water contact angle from approximately 112° to 87°, indicating increased wettability of the nanofibrous structures. SEM analysis showed that silica incorporation did not significantly alter fiber morphology, with only minor defects being observed (Figure 6). Increased wettability may favour cell-material interactions and support applications such as tissue engineering and in vitro cell culture systems. PA6 nanofibers incorporating silica particles exhibited limited changes in overall fiber morphology following electrospinning processing. SEM analysis revealed the presence of bulged structures associated with particle encapsulation within the polymeric matrix (Figure 7). The incorporation of silica did not significantly affect the hydrophobic behaviour of the fibers, likely due to complete particle coverage by polymer chains. Such nanofibrous systems may be suitable for applications requiring breathable fibrous barriers, including filtration systems and wound dressing platforms. Antimicrobial activity was preserved after incorporation of multifunctional silica particles into electrospun fibers. Contact-based antimicrobial assays demonstrated inhibitory effects against *Staphylococcus aureus* in formulations containing antimicrobial particles, confirming that the electrospinning process did not compromise particle functionality. The incorporation of multifunctional silica particles (SiO_2_RHSK_MF) into electrospun systems may additionally contribute to protective textile applications due to the antimicrobial and flame-retardant functionalities associated with the particles. Such multifunctional nanofibrous structures

could support the development of advanced protective coatings, technical textiles and protective apparel systems.

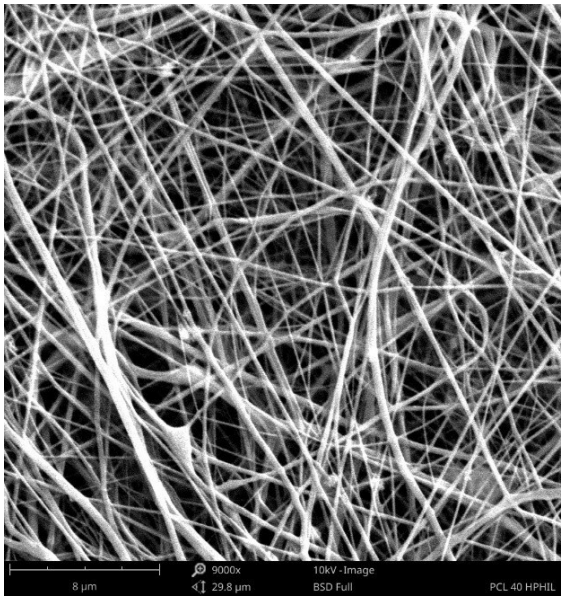


Figure 6: Morphology of PCL nanofibers with hydrophilic silica particles 40wt%

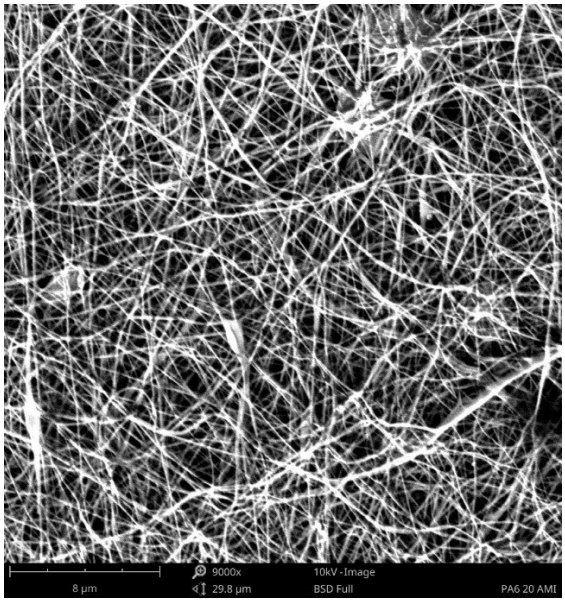


Figure 7: Morphology of PA6 nanofibers with 20 wt% of antimicrobial biosilica particles.

4 CONCLUSIONS

High purity SiO_2_RHSK was recovered from rice husk ash using alkaline digestion followed by neutralization and washing steps, producing particles with morphology and size distributions suitable for further surface treatment and incorporation into polymer solutions. Surface functionalization with a quaternary ammonium silane and a phosphorus containing flame retardant agent was successfully achieved, as confirmed by different physical and chemical characterization analysis, as well as the increased hydrophobicity and flame retardancy.

The SiO_2_RHSK_MF has shown promising results in reducing the growth of *E. coli* and *S. aureus*. Contact angle measurements demonstrated an increase in water repellence after the modification of the particles' surface, and preliminary flame retardancy screening revealed that after 10 seconds of flame exposure, the flame was extinguished, confirming the flame-retardant behaviour.

The incorporation of the modified particles into electrospun polymer matrices was accomplished after optimization of solution and processing parameters such as the applied voltage, flow rate, and the types of electrospinning collectors and electrodes. The resulting nanofibrous meshes exhibited uniform structure (e.g., thickness, porosity), which indicates a successful integration of SiO_2_RHSK particles in polymer fibres. Moreover, the integration of modified particles conferred unique properties (e.g., antimicrobial, hydrophobic) to the electrospun membranes, making them suitable for scaling up and for several commercial applications.

Overall, the results demonstrate that biosilica from rice husk can be converted into a multifunctional filler whose tailored surface chemistry translates into antimicrobial, hydrophobic and flame-retardant performance when integrated into electrospun nanofibers, without compromising fiber morphology or manufacturability.

5 REFERENCES

[1] Kirchherr, J.; Reike, D.; Hekkert, M. Conceptualizing the circular economy: An analysis of 114 definitions. Resour. Conserv. Recycl. 2017, 127, 221–232. https://doi.org/10.1016/j.resconrec.2017.09.005

[2] Hazen, B.T.; Mollenkopf, D.A.; Wang, Y. Remanufacturing for the Circular Economy: An Examination of Consumer Switching Behavior. Bus. Strateg. Environ. 2017, 26, 451–464. https://doi.org/10.1002/bse.1929

[3] Geisendorf, S.; Pietrulla, F. The circular economy and circular economic concepts—a literature analysis and redefinition. Thunderbird Int. Bus. Rev. 2018, 60, 771–782. https://doi.org/10.1002/tie.21924

[4] Mofijur, M.; Mahlia, T.M.I.; Logeswaran, J.; Anwar, M.; Silitonga, A.S.; Rahman, S.M.A.; Shamsuddin, A.H. Potential of Rice Industry Biomass as a Renewable Energy Source. Energies 2019, 12, 4116. https://doi.org/10.3390/en12214116

[5] Siddique, R. Rice Husk Ash. In Waste Materials and By-Products in Concrete; Springer Berlin Heidelberg: Berlin, Heidelberg, 2008; pp. 235–264. ISBN 978-3-54074294-4.

[6] Jongpradist, P.; Homtragoon, W.; Sukkarak, R.; Kongkitkul, W.; Jamsawang, P. Efficiency of Rice Husk Ash as Cementitious Material in High-Strength Cement Admixed Clay. Adv. Civ. Eng. 2018, 2018, 8346319. https://doi.org/10.1155/2018/8346319

[7] Rajanna, S.K.; Kumar, D.; Vinjamur, M.; Mukhopadhyay, M. Silica Aerogel Microparticles from Rice Husk Ash for Drug Delivery. Ind. Eng. Chem. Res. 2015, 54, 949–956. https://doi.org/10.1021/ie503867p

[8] Alshatwi, A.A.; Athinarayanan, J.; Periasamy, V.S.

Biocompatibility assessment of rice husk-derived biogenic silica nanoparticles for biomedical applications. Mater. Sci. Eng. C 2015, 47, 8–16. https://doi.org/10.1016/j.msec.2014.11.005

[9] Zhang, C.; Kang, H.; Lv, K.; Chen, H.; Yuan, S. Maize Phytoliths and Photoluminescent Silica Nanotubes Prepared from a Natural Silica Resource. Ind. Eng. Chem. Res. 2011, 50, 12521–12526. https://doi.org/10.1021/ie2003768

[10] Adam, F.; Appaturi, J.N.; Iqbal, A. The utilization of rice husk silica as a catalyst: Review and recent progress. Catal. Today 2012, 190, 2–14. https://doi.org/10.1016/j.cattod.2012.04.056

[11] Sekifuji, R.; Tateda, M. Study of the feasibility of a rice husk recycling scheme in Japan to produce silica fertilizer for rice plants. Sustain. Environ. Res. 2019, 29, 11. https://doi.org/10.1186/s42834-019-0011-x

[12] Hossain, S.K.S.; Mathur, L.; Roy, P.K. Rice husk/rice husk ash as an alternative source of silica in ceramics: A review. J. Asian Ceram. Soc. 2018, 6, 299–313. https://doi.org/10.1080/21870764.2018.1539210

[13] Mohd Daud, F.D.; Azmy, N.A.M.; Mahmud, M.S.; Sariffudin, N.; Zaki, H.H.M. Preparation of Nanosilica Powder Using Rice Husk via Precipitation Method. Mater. Sci. Forum 2020, 1010, 501–507. https://doi.org/10.4028/www.scientific.net/MSF.1010.51

[14] Yuvakkumar, R.; Elango, V.; Rajendran, V.; Kannan, N. High-purity nano silica powder from rice husk using a simple chemical method. J. Exp. Nanosci. 2014, 9, 272–281. https://doi.org/10.1080/17458080.2012.656709

[15] Song, J.; Kong, H.; Jang, J. Bacterial adhesion inhibition of the quaternary ammonium functionalized silica nanoparticles. Colloids Surf. B Biointerfaces 2011, 82, 651–656. https://doi.org/10.1016/j.colsurfb.2010.10.027

[16] Gong, S.; Epasinghe, D.J.; Zhang, W.; Zhou, B.; Niu, L.; Ryou, H.; Eid, A.A.; Frassetto, A.; Yiu, C.K.Y.; Arola, D.D.; et al. Synthesis of antimicrobial silsesquioxane–silica hybrids by hydrolytic co-condensation of alkoxysilanes. Polym. Chem. 2014, 5, 454–462. https://doi.org/10.1039/C3PY00635B

[17] Wang, X.; Shi, L.; Zhang, J.; Cheng, J.; Wang, X. Self-assembly fabrication microstructures and antibacterial performance of layer-structured montmorillonite nanocomposites with cationic silica nanoparticles. RSC Adv. 2017, 7, 31502–31511. https://doi.org/10.1039/C7RA04353H

[18] Tomšič, B.; Ilec, E.; Žerjav, M.; Hladnik, A.; Simončič, A.; Simončič, B. Characterisation and functional properties of antimicrobial bio-barriers formed by natural fibres. Colloids Surf. B Biointerfaces 2014, 122, 72–78. https://doi.org/10.1016/j.colsurfb.2014.06.047

[19] Vasiljević, J.; Tomšič, B.; Jerman, I.; Orel, B.; Jakša, G.; Simončič, B. Novel multifunctional water- and oil-repellent, antibacterial, and flame-retardant cellulose fibres created by the sol–gel process. Cellulose 2014, 21, 2611–2623. https://doi.org/10.1007/s10570-014-0293-4

[20] [20] Vasiljević, J.; Zorko, M.; Štular, D.; Tomšič, B.; Jerman, I.; Orel, B.; Medved, J.; Kovač, J.; Simončič, B. Structural optimisation of a multifunctional water- and oil-repellent, antibacterial, and flame-retardant sol–gel coating on cellulose fibres. Cellulose 2017, 24, 1511–1528. https://doi.org/10.1007/s10570-016-1187-4

[21] Riaz, S.; Ashraf, M.; Hussain, T.; Hussain, M.T. Modification of silica nanoparticles to develop highly durable superhydrophobic and antibacterial cotton fabrics. Cellulose 2019, 26, 5159–5175. https://doi.org/10.1007/s10570-019-02440-x

[22] Cheng, X.-W.; Tang, R.-C.; Guan, J.-P.; Zhou, S.-Q. An eco-friendly and effective flame-retardant coating for cotton fabric based on phytic acid doped silica sol approach. Prog. Org. Coat. 2020, 141, 105539. https://doi.org/10.1016/j.porgcoat.2020.105539

[23] Barbalini, M.; Bertolla, L.; Toušek, J.; Malucelli, G. Hybrid Silica-Phytic Acid Coatings: Effect on the Thermal Stability and Flame Retardancy of Cotton. Polymers (Basel) 2019, 11, 1664. https://doi.org/10.3390/polym11101664

[24] Sui, Y.; Qu, L.; Dai, X.; Li, P.; Zhang, J.; Luo, S.; Zhang, C. A green self-assembled organic supermolecule as an effective flame retardant for epoxy resin. RSC Adv. 2020, 10, 12492–12503. https://doi.org/10.1039/D0RA00072H

[25] Fu, J.; Yang, F.; Chen, G.; Zhang, G.; Huang, C.; Guo, Z. A facile coating with water-repellent and flame-retardant properties on cotton fabric. New J. Chem. 2019, 43, 10183–10189. https://doi.org/10.1039/C9NJ02240F

[26] Keirouz, A.; Wang, Z.; Reddy, V.S.; Nagy, Z.K.; Vass, P.; Buzgo, M.; Ramakrishna, S.; Radacsi, N. The History of Electrospinning: Past, Present, and Future Developments. Adv. Mater. Technol. 2023, 8, 2201723. https://doi.org/10.1002/admt.202201723

[27] Omer, S.; Forgách, L.; Zelkó, R.; Sebe, I. Scale-up of Electrospinning: Market Overview of Products and Devices for Pharmaceutical and Biomedical Purposes. Pharmaceutics 2021, 13, 286. https://doi.org/10.3390/pharmaceutics13020286

[28] Tsareva, A.D.; Shtol, V.S.; Klinov, D.V.; Ivanov, D.A. Electrospinning for Biomedical Applications: An Overview of Material Fabrication Techniques. Surfaces 2025, 8, 7. https://doi.org/10.3390/surfaces8010007

[29] Al-Abduljabbar, A.; Farooq, I. Electrospun Polymer Nanofibers: Processing, Properties, and Applications. Polymers 2023, 15, 65. https://doi.org/10.3390/polym15010065

[30] Khlebtsov, B.N.; Burov, A.M. Synthesis of Monodisperse Silica Particles by Controlled Regrowth. Colloid J. 2023, 85, 456–468. https://doi.org/10.1134/S1061933X23600379

[31] Croissant, J.G.; Fatieiev, Y.; Almalik, A.; Khashab, N.M. Mesoporous silica and organosilica nanoparticles: physical chemistry, biosafety, delivery strategies, and biomedical applications. Adv. Healthcare Mater. 2018, 7, 1700831. https://doi.org/10.1002/adhm.201700831

[32] Ahmadi Bonakdar, M.; Rodrigue, D. Electrospinning: Processes, Structures, and Materials. Macromol 2024, 4, 58–103. https://doi.org/10.3390/macromol4010004

[33] Peranidze, K.; Safronova, T.V.; Kildeeva, N.R. Electrospun Nanomaterials Based on Cellulose and

Its Derivatives for Cell Cultures: Recent Developments and Challenges. Polymers 2023, 15, 1174. https://doi.org/10.3390/polym15051174

[34] Zhang, J.; Yu, M.; Tao, S. Advanced electrospinning nanomaterials: From spinning fabrication techniques to electrochemical applications. Nano Res. 2024, 17, 7077–7116. https://doi.org/10.1007/s12274-024-6753-8

[35] Pode, R. Potential applications of rice husk ash waste from rice husk biomass power plant. Renew. Sustain. Energy Rev. 2016, 53, 1468–1485. https://doi.org/10.1016/j.rser.2015.09.051

[36] Aguilar, H.; Barros, A.; Ornelas, M.; Malgueiro, R.; Carvalho, A.; Portela, A.; Silva, C.; Grishchuk, S.; Gryshchuk, L.; Gilberg, M.; et al. Use of biogenic silica nanoparticles derived from biomass in polymeric formulations and their applications. Mater. Compos. 2020, 4, 22–28. ISSN: 2531-0739.

[37] Yudovin-Farber, I.; Beyth, N.; Weiss, E.I.; Domb, A.J. Antibacterial effect of composite resins containing quaternary ammonium polyethyleneimine nanoparticles. J. Nanoparticle Res. 2010, 12, 591–603. https://doi.org/10.1007/s11051-009-9628-8

[38] Zhang, R.; Cai, S.; Xu, G.; Zhao, H.; Li, Y.; Wang, X.; Huang, K.; Ren, M.; Wu, X. Crack self-healing of phytic acid conversion coating on AZ31 magnesium alloy by heat treatment and the corrosion resistance. Appl. Surf. Sci. 2014, 313, 896–904. https://doi.org/10.1016/j.apsusc.2014.06.104

[39] Rafique Ullah; Biplob Kumer Deb; M.Y.A.M. Synthesis and Characterization of Silica Coated Iron-Oxide Composites of Different Ratios. Int. J. Compos. Mater. 2014, 4, 2166–4919. https://doi.org/10.5923/j.cmaterials.20140402.13

[40] Li, K.M.; Jiang, J.G.; Tian, S.C.; Chen, X.J.; Yan, F. Influence of silica types on synthesis and performance of amine-silica hybrid materials used for CO2 capture. J. Phys. Chem. C 2014, 118, 2454–2462. https://doi.org/10.1021/jp408354r

[41] Gong, S.; Epasinghe, D.J.; Zhang, W.; Zhou, B.; Niu, L.; Ryou, H.; Eid, A.A.; Frassetto, A.; Yiu, C.K.Y.; Arola, D.D.; et al. Synthesis of antimicrobial silsesquioxane–silica hybrids by hydrolytic co-condensation of alkoxysilanes. Polym. Chem. 2014, 5, 454–462. https://doi.org/10.1039/C3PY00635B

[42] Wang, X.; Shi, L.; Zhang, J.; Cheng, J.; Wang, X. Self-assembly fabrication microstructures and antibacterial performance of layer-structured montmorillonite nanocomposites with cationic silica nanoparticles. RSC Adv. 2017, 7, 31502–31511. https://doi.org/10.1039/C7RA04353H

[43] Rauner, N.; Mueller, C.; Ring, S.; Boehle, S.; Strassburg, A.; Schoeneweiss, C.; Wasner, M.; Tiller, J.C. A Coating that Combines Lotus-Effect and Contact-Active Antimicrobial Properties on Silicone. Adv. Funct. Mater. 2018, 28, 1801248. https://doi.org/10.1002/adfm.201801248

[44] Yilbas, B.S.; Yousaf, M.R.; Al-Sharafi, A.; Ali, H.; Al-Sulaiman, F.; Abu-Dheir, N.; Khaled, M.; Al-Aqeeli, N. Silicone oil impregnated nano silica modified glass surface and influence of environmental dust particles on optical transmittance. RSC Adv. 2017, 7, 29762–29771. https://doi.org/10.1039/C7RA03392C

6 ACKNOWLEDGEMENTS

The PRIMED project has received funding from the European Union's HORIZON programme under grant agreement N°101135353.